Journal of Rehabilitation in Civil Engineering 8-4 (2020) 90-105

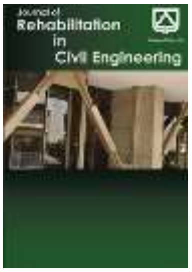

journal homepage: http://civiljournal.semnan.ac.ir/

Experimental Study of Masonry Structure under Impact Loading and Comparing it with Numerical Modeling Results via Finite Element Model Updating

M. Malekshahi [1] and A.H. Akhaveissy [2*]

1. PhD student, Department of Civil Engineering, Razi University, Kermanshah, Iran
2. Associate professor, Department of Civil Engineering, Razi University, Kermanshah, Iran

Corresponding author: *ahakhaveissy@razi.ac.ir*

ARTICLE INFO

Article history:
Received: 02 April 2019
Accepted: 24 May 2020

Keywords:
Finite element model updating;
Close-in explosion;
Underground explosion;
Unreinforced masonry structure.

ABSTRACT

Given the sophisticated nature of the blast phenomenon in relation to structures, it is of significance to accurately investigate the structure behavior under blast loads. Due to its rapid and transient nature, blast loading is one of the most important dynamic loadings on the structures. Since masonry materials are widely used as the partition and bearing walls in the existing and newly-built structures, the current research aims to investigate the buried blast effects on unreinforced masonry structures. In order to apply the blast load on a crater as time history, it is required to determine the maximum free field pressure caused by the blast. Accordingly, Finite Element Model Updating (FEMU) was used to calculate the maximum free-field pressure. Thus, for a non-linear dynamic analysis of a blast-loaded structure, a code written in FORTRAN was used. Mohr-Coulomb yield surface with tensile and compression cap and classic Mohr-Coulomb yield surface were used for the structure and the soil modeling, respectively. The comparison of the numerical analysis results in FEMU to field data shows a good consistency between the numerical results and the field data.

1. Introduction

An important issue in passive defense has always been the structure reinforcement against blast loads. The first step on this path is to identify and model the blast effects on structures. Given the vulnerability of these buildings to vibration, study of the behavior and performance of masonry buildings in response to the blast loads must be taken into account.

Since the recent decades, varied research has been performed on numerical modeling to explore the blast details and to foresee the relevant structure responses [1]. Thus, it is of necessity to recognize the dynamic response of structures under blast loading in order to

DOI: 10.22075/JRCE.2020.17519.1333

safeguard the structures against explosions [2]. Recently, researchers have conducted an extensive body of research on the dynamic response of masonry structures under blast. For instance, some researchers investigated the nonlinear dynamic response of masonry walls subjected to explosion via a three-dimensional model in which brick and mortar are modeled separately [3-7]. This method is able to produce accurate responses by using the appropriate model with the exact parameters and considering the interface between bricks and mortar. However, the numerical model is highly intricate and its analysis requires a considerable amount of time. Some researchers [8-11] proposed a homogeneous method for masonry material, which can be used for simulating the dynamic response of masonry structure subjected to explosion. Keys and Clubley [12] studied masonry wall parts under explosive loads based on the Applied Element Method (AEM). The results indicated an appropriate relationship between the field and numerical results. Riedel et al. [13] examined the nonlinear response of masonry walls with openings under explosive charges. Blast loads include bomb and explosive gas. Akhaveissy et al. [14] proposed a nonlinear finite element method based on the modified generalized plasticity model for soil behavior modeling considering hardening-softening and used a Disturbed State Concept (DSC) with a Hierarchical Single-Surface (HISS) yield surface. Akhaveissy [15, 16] implemented the generalized plasticity method for soil-structure interaction modeling. The comparison of the results indicated that there is a significant relationship between experimental data and numerical model.

However, the interaction of soil and masonry structures under blast was not taken into account in the previous studies. On the other hand, researchers did not focus on the structure acceleration under substructure blast, which can provide engineers and researchers with effective data. As a significant numerical modeling method, finite element method has contributed to exact and satisfactory results. However, in some cases, the results obtained from the method have not been consistent with experimental results. Thus, it is required to find a method to minimize the difference between analysis and experimental results. Zhenguo and Yong Lu [17] used the genetic algorithm to reduce the difference between theoretical and experimental frequencies. In the research, optimal location of artificial boundaries was determined via FEMU. Zuo-Cai Wang et al. [18] proposed a nonlinear update method based on the amplitudes and frequencies of the dynamic response. The objective function was developed based on the difference between the experimental frequencies and the frequency obtained from the nonlinear model. The proposed method effectively updates the nonlinear model, and the presence of noise has slight impact on the updating procedure. Yalan Xu et al. [19] presented a damage detection method based on the probabilistic approach. After modifying the optimization algorithm, the researchers investigated a plane truss, and compared the results using the Monte Carlo simulation. The results indicated the correct identification of damaged members in the truss.

Bakir et al. [20] used sensitivity viewpoints in calibration, and applied a constrained optimization method to minimize differences between natural frequencies and figures' mode. In numerical modeling of masonry structures, particularly for historical masonry structures, it is necessary to take into account the inevitable lack of knowledge and the effects of unknown parameters (*i.e.* material properties, geometry, boundary conditions, etc.). Therefore, using experimental data, Bartoli et al. [21] proposed a Bayesian method in their research for the FEM Updating of the masonry towers. Schlune et al. [22] used calibration of the finite element model to improve the assessment of bridges. The research aimed to eliminate simplified modeling errors through physical model corrections prior to the parameter approximation through nonlinear optimization. In addition, multi- response objective functions were developed and allowed to use a combination of different types of measurements to achieve a reliable method in parameter estimation. Huang and Zhu [23] used optimization methods for the calibration of the finite element model relevant to bridge structures. The results showed that the FEM Updating reflects the bridge's dynamic characteristics more accurately and provides the basis for the theory to identify and monitor the bridge damages.

Therefore, the FEM Updating is used to minimize the difference between analysis and experimental results.

Three-dimensional finite element program was written in FORTRAN for non-linear dynamic analysis of the masonry structure under blast loading. The present research attempts to provide a macro model for masonry structure assessment. Thus, Mohr-Coulomb yield surface with a tensile and compression cap was used for accurate masonry structure analysis, while classic Mohr-Coulomb yield surface was used for soil modelling. Given the above statements and reviewing the research literature, it can be concluded that masonry structure behavior modeling under blast-driven vibration by the FEM Updating needs further investigations. Thus, performing experimental researches and numerical modeling, the present study examines masonry structure behavior under blast load using the FEM Updating.

2. Experiment Scheme

As shown in Figure 1, the structure dimensions within the plan are 1.5m × 1m.The bottom opening has a width of 0.4 m and a height of 0.8 m, and the above opening has a width of 0.4 m and a height of 0.5 m.

The unreinforced walls had 2.2×1×0.1m of dimensions, and were loaded by blast ignited from 4.5kg of ammonium nitrate (ANFO) and 0.428 kg of gel-dynamite (Emulite) that was equivalent to 3.98kg of TNT [24]. The blast location was 2m from the structure center, 1.5m lower than the ground.

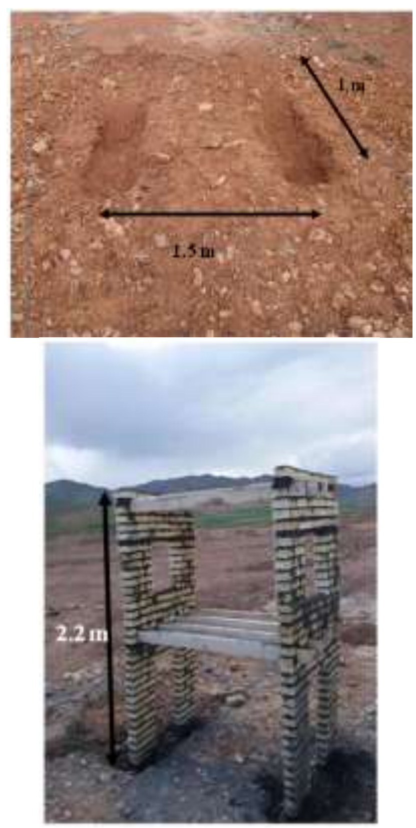

(a)

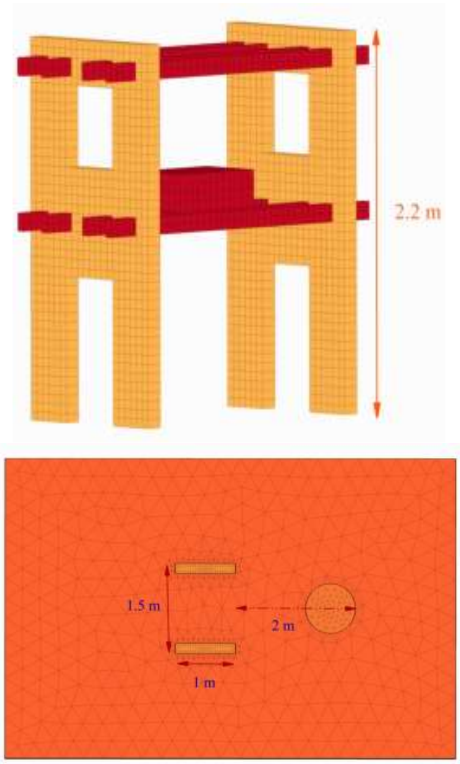

(b)

Fig. 1. Construction process,(a) site of experiment, (b) schematic shape.

For each floor, 4 woods with 0.1×0.05m cross-section were used. The woods had 1.7m of length.

Young’s modulus and Poisson's ratio of the timbers were 11000 MPa and 0.3, respectively, and their mass per unit was 900 Kg/m^3.

The masonry walls were constructed at the site and each specimen had to be cured. The thickness of the mortar is 10 mm. As displayed in Figures 2 and 3, four samples were fabricated to calculate the compressive strength and tensile strength of the masonry unit. Table 1 indicates the results of the experiments.

Fig. 2. Compression Strength Experiment

Fig. 3. Tensile Strength Experiment.

In the experiment 1, the shear and flexural anchor values were calculated following the sample loading at the failure point. After determining the shear stress and normal stress, the tensile strength of the sample was calculated to be 0.29 MPa by using Mohr’s circle. Then, as shown in Table 1, the tensile strength values were determined for other specimens after performing the tests and necessary calculations.

Table 1. Compressive strength and tensile strength of the unit.

Sample	Compressive strength (MPa)	Average of compressive strength (MPa)	Tensile strength (MPa)	Average of tensile strength (MPa)
1	3.1	**3.625**	0.29	**0.34**
2	3.5		0.31	
3	3.8		0.36	
4	4.1		0.4	

Based on the average sample strength, the compressive and tensile strength of the masonry blocks was determined to be 3.7 MPa and 0.34 MPa, respectively.

Triaxial experiments were performed under CU mode to determine the mechanical parameters of the soil according to ASTM D4967 [25].

3. Instrumenta and Principles

As mentioned earlier, a parameter taken into account in the present study was the acceleration induced by the blast on the structure wall. Accelerometer sensors were used to measure the acceleration. The sensors were connected to a dynamic data logger via cables and proper connections. The sensors were able to measure the acceleration in one or two directions. The acceleration and sensor resonance frequency were 50g and 5.5 kHz, respectively. A four-channel data logger was utilized that had the ability to record 250 MSa/sec signals with 12 bit of clarity. The cables were 40m long without voltage loss.

Three accelerometer sensors including A_1, A_2, and A_3 with the above-mentioned features were utilized in the test. Accelerometers were installed on the down, middle and top of the wall to record the acceleration acting on the structure. Figure 4 illustrates the detailed locations of the sensors A_1, A_2, and A_3.

Figure 5 shows the blast process at the beginning and the end of the blast.

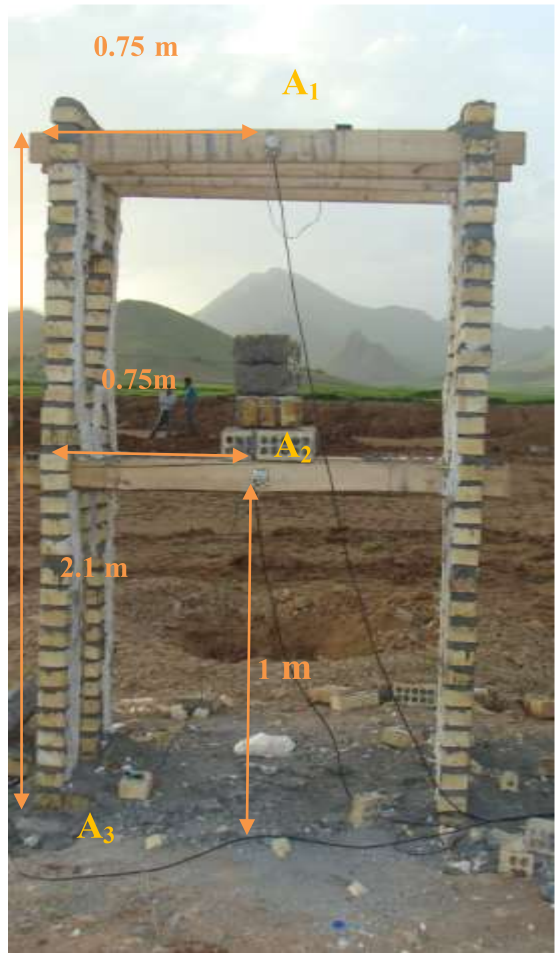

Fig. 4. The sensors position.

No one was allowed to enter the area when the explosives were detonated and all systems were monitored from a safe position. The distance of the scale was $1.26\, m/kg^{1/3}$, indicating that the explosion was carried out in the near field. Figure 5 shows the explosion process at the beginning and end of the explosion.

(a) the beginning of the blast.

(b) the end of the blast.

Fig.5. Blast Process; (a) Beginning and (b) End of the explosion.

4. Numerical Simulation

Numerical simulation through computational models has traditionally been regarded as an appropriate tool in the structure designing process. The soil behavior is linear in small deformation while it becomes non-linear in heavy loads, especially blast loads [26, 27].

Regarding the features related to Mohr-Coulomb model, this model was used for expressing the non-linear behavior of soil [28-30].

Table 2 represents the mechanical properties of the soil extracted from drilling bore holes at the study site. Figure 6 indicates the cross-section of the structure and the crater location.

Table 2. Soil Properties.

Materials	Properties	Unit	Value
Soil 1	**Mass per unit**	**Kg/m^3**	**1850**
	Cohesion	**MPa**	**0.015**
	Friction angle	**Degree**	**35**
	Dilatancy angle (ψ)	**Degree**	**35**
	Young's modulus	**MPa**	**80**
Soil 2	**Mass per unit**	**Kg/m^3**	**1850**
	Cohesion	**MPa**	**0.005**
	Friction angle	**Degree**	**30**
	Dilatancy angle (ψ)	**Degree**	**30**
	Young's modulus	**MPa**	**50**

Soil 1 is meant to be the undisturbed soil surrounding the building structure, and the characteristics of the soil spilled over the buried crater is indicative of the soil 2, as seen in Table 3.

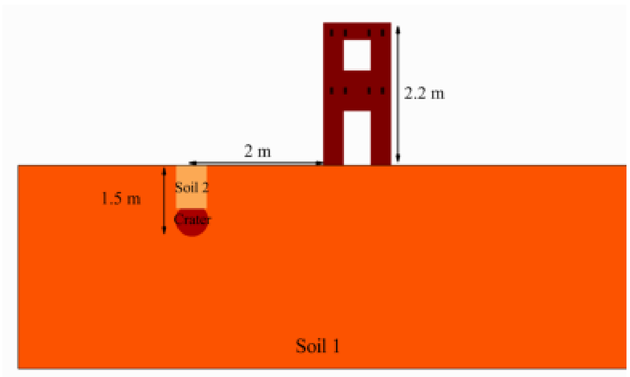

Fig. 6. Structure Cross-Section and Explosive Materials Location (Crater).

4.1. Masonry Structure Modeling

The first step in the seismic structure assessments and reinforcement schemes is structure modelling. Various numerical models applicable to the masonry structure behavior simulations require several parameters necessitating costly and unnecessary experiments along with operational knowhow. The current research seeks to provide a macro model using simple and conventional test results for masonry wall assessment. In the research, a macro model was presented for the masonry structure evaluation. In macro modeling, the brick wall is assumed to be a homogeneous and uniform material with equivalent mechanical properties. The modeling in this method is simple, and the computation volume is much lower than the micro modeling. Thus, Mohr-Coulomb yield surface with a compression and tensile cap was used for the accurate masonry structure analysis (Figure 7).

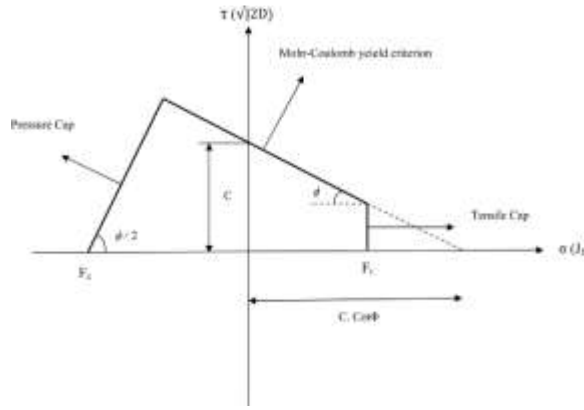

Fig. 7. Mohr-Coulomb Yield Surface with Compression and Tensile Cap.

In the modeling, the soil boundary on the sides, front and rear of the structure is 2150 mm, 4500 mm and 3500 mm, respectively. The distance was determined based on the analysis and non-interference of the underground blast waves. According to Figure 8, a 3-D numerical model was provided to predict the response of the structure under the blast loading. 70kg was considered as the gravity load of the floor 1. Young’s modulus and Poisson's ratio of the structure were1600 MPa and 0.2, respectively, and the structure specific weight was 1800 Kg/m^3. The behavior of the timbers in the modeling was considered linear.

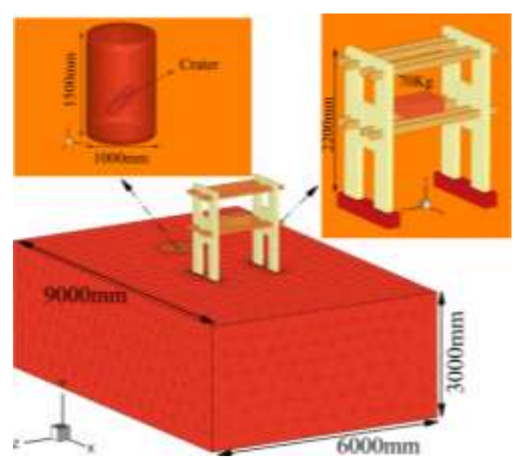

Fig. 8. 3-D View of Structure, Soil, and Crater Modeling.

It is noteworthy that the Coulomb Mohr criterion behavior is completely elasto-plastic, and since the macro method is used for the masonry structure modelling, the material softening behavior of the materials (same as concrete) should be taken into account in the modeling.

Exposing to tensile stress up to the point of cracking resistance (i.e. tensile cut-off), the masonry materials behave elastically. Then, with increasing the plastic strain, tensile strength amount is reduced. Based on a number of tests carried out on masonry materials, the following mathematical equations are presented [31].

For the compressive behavior:

Eq. (1.a) relates to the Hognestad's model

$$f_m = \begin{cases} f'_m\left[2(\frac{\varepsilon}{\varepsilon_o})-(\frac{\varepsilon}{\varepsilon_o})^2\right] & \varepsilon \le \varepsilon_o \quad (1.a) \\ f'_m(1-0.15(\frac{\varepsilon-\varepsilon_0}{\varepsilon_{cu}-\varepsilon_o})) & \varepsilon_0 < \varepsilon \le \varepsilon_1 \quad (1.b) \\ 0.2 f'_m & \varepsilon > \varepsilon_1 \quad (1.c) \end{cases}$$

on the compressive behavior of concrete, which can be used in modeling of the compressive test of the masonry block. Eq. (1.b) is a linear function between the maximum stress and the residual stress within the softening region. The Eq. (1.c) is the residual stress assumed to be 20% of the maximum stress.

For the tensile behavior:

$$f_t = \begin{cases} E_c\varepsilon & \varepsilon \le \varepsilon_t \quad (2.a) \\ \lambda f_m'(1-\frac{\varepsilon-\varepsilon_t}{\varepsilon_m-\varepsilon_t}) & \varepsilon > \varepsilon_t \quad (2.b) \end{cases}$$

The Eq. (2.a) indicates the tensile behavior within the elastic region, and the Eq. (2.b) is applied to the softening region. In these equations, f'_m is the compressive strength of the masonry prism, and we have $0.002 \le \varepsilon_o \le 0.004$ and $0.003 \le \varepsilon_{cu} \le 0.007$. Further, $\varepsilon_m = 10\varepsilon_t$ and λ varies from 0.1 to 0.25. E_c is the modulus of elasticity of the masonry unit, and ε_1 and ε_t are shown in Figure 9.

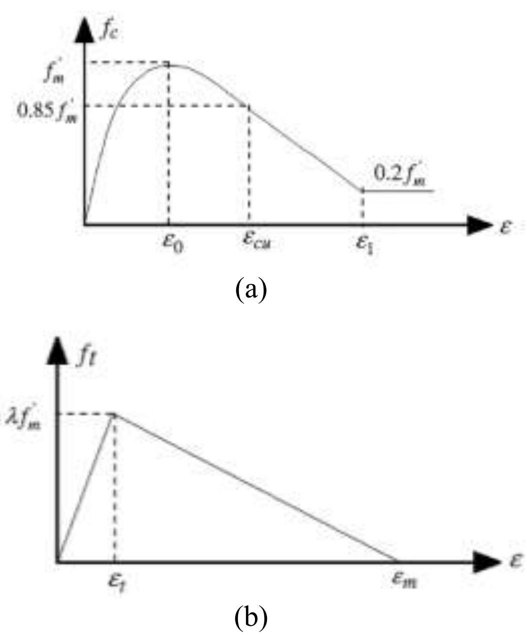

Fig. 9. The behavior of the masonry prism, a) for compression, b) for tension [31].

4.2. Explosive Load Modeling

The blast loads can be expressed as a pressure with a time pressure diagram in the exponential or triangle form that promptly abates in terms of magnitude and range. The shock wave steadily reduces from P_0 to almost zero according to the following equation.

$$P_t = P_0 e^{-t/t_a} \tag{3}$$

Where P_0 denotes the maximum blast pressure in the free field, P_t is the blast pressure at the time *t*, and t_a is the time the shock wave takes to be applied to a given location of the structure. It is calculated from the following equation.

$$t_a = \frac{R}{C} \tag{4}$$

In which R is the blast location distance from the structure and C denotes the blast wave velocity in the soil.

P_0 is introduced by the U.S. Army as [32],

$$P_0 = 48.8\rho.c(\frac{2.52R}{W^{1/3}})^{-n} \tag{5}$$

Where ρ indicates the mass per unit of the soil (1850 Kg/m^3), C represents the wave velocity, R is regarded as the standoff distance from the crater (2m), W is described as the weight of explosive charge (3.98 Kg), f_c is coupling factor and n denotes the damping coefficient [32].

According to Eq. 5, P_0 is calculated as 1.175 MPa. It is worth noting that according to the U.S. Army Code [32], a pre-compression has to be applied to the structure. However, no equation has been provided in explosion charge modeling to calculate the overpressure on the crater. Thus, the FEM Updating is used in this study to determine the maximum compression of the free field and apply it to the crater. Figure 10 shows the blast pressure history curve.

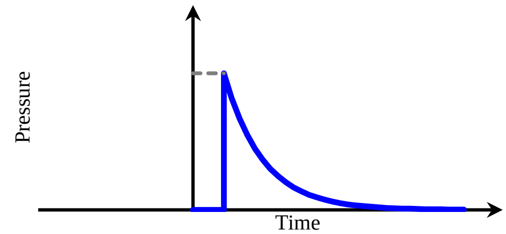

Fig. 10. Pressure-time history curve of blast.

Figure 10 shows the pressure-time history graph of explosion. The shock forehead is called the blast wave that is determined by a pressure escalating into the maximum pressure P_0.

The increase in the pressure distributes radially to the maximum shock, with the blast point velocity reducing gradually. In the buried blast, energy propagates in the form of pressure and shear waves in the ground, producing new shocks that can bring about significant destructive effects.

5. Comparison of Numerical Results with Field Data

The engineers' principal concern is to examine the performance of the structures in response to gravity and lateral loads. Various studies have been conducted on seismic loads. The results have continuously been edited, and published in the form of design codes. However, the blast loads that are applied more rapid than earthquake by almost 1000 times are relatively unknown. Thus, due to the more focus on the passive defense, blast research has received an increasing attention in the recent years. First, the validity of the FEM code was evaluated. To this end, the model's ability to present the masonry materials behavior was assessed using the parameters in Table 3. This assessment is done for a stress point using the integration of constitutive equations.

Table 3. Mechanical Properties of Masonry Unit [31].

Material	Parameters					
Masonry unit	$f'_m(MPa)$	$f_t(MPa)$	$E(MPa)$	ϕ	$C(MPa)$	ν
	3	0.1	1650	26.56	0.15	0.2

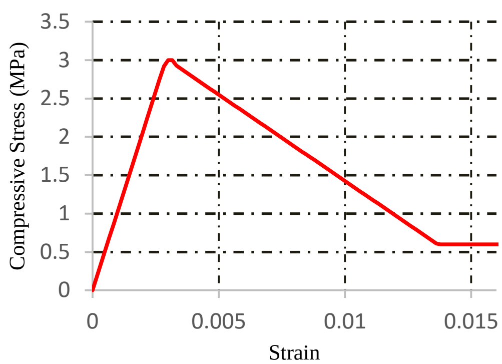

(a)

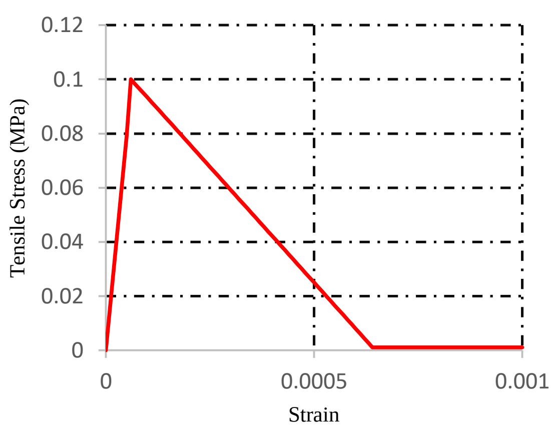

(b)

Fig.11. Strain-strain diagram model for:

(a) compressive and (b) tensile behavior of a masonry unit.

According to Figure11, the numerical model results properly represent the structure behavior that is based on analytical uniaxial compression-tension curves (equations 1 to 5). In the following, a computer program is run to analyze the blast-driven masonry structure.

As mentioned earlier, in the current study, the dynamic response of the unreinforced masonry structure is investigated under near-field blast event. To this end, the field study of the masonry structure was investigated. Macro method was used to model the masonry materials in this study. The brick wall was homogenous and uniform in terms of mechanical properties. The weight of the explosive was tantamount to 3.98 TNT kg. The explosive was located 2 meters away from the center of the building and 1.5 meters under the ground. In the modeling, both the base structure and the lower part of the soil surrounding the structure were fixed, and the soil edges were bounded in the horizontal direction and could only move in the vertical direction. Figures. 12a, 12b, and 12c represent the accelerations recorded by the sensors.

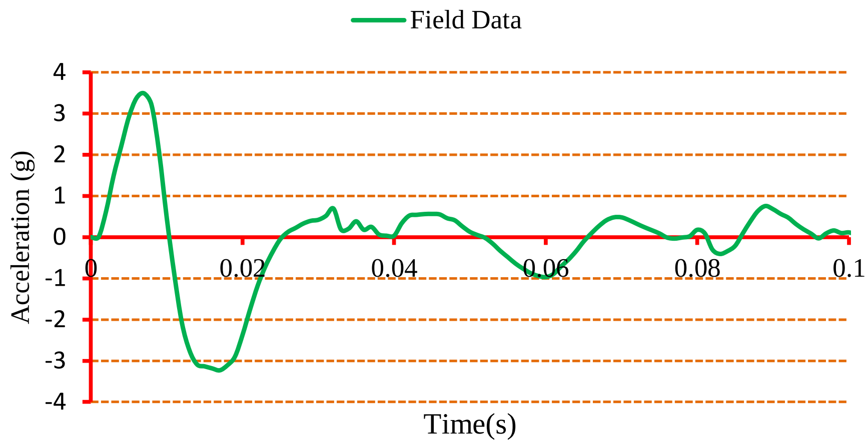

(a)

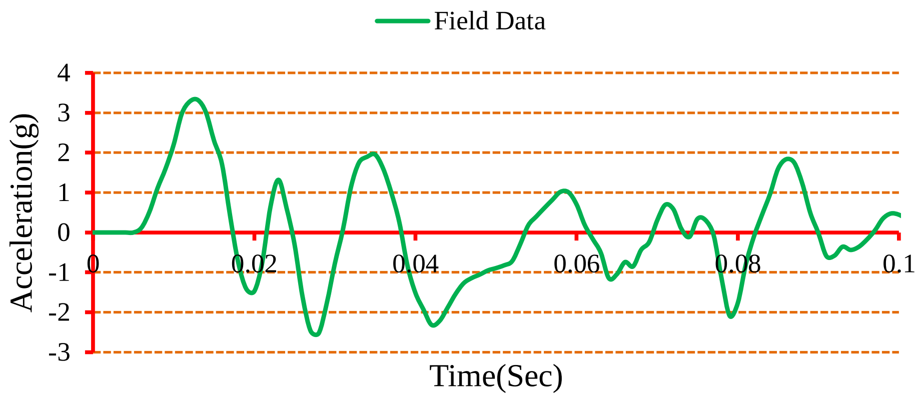

(b)

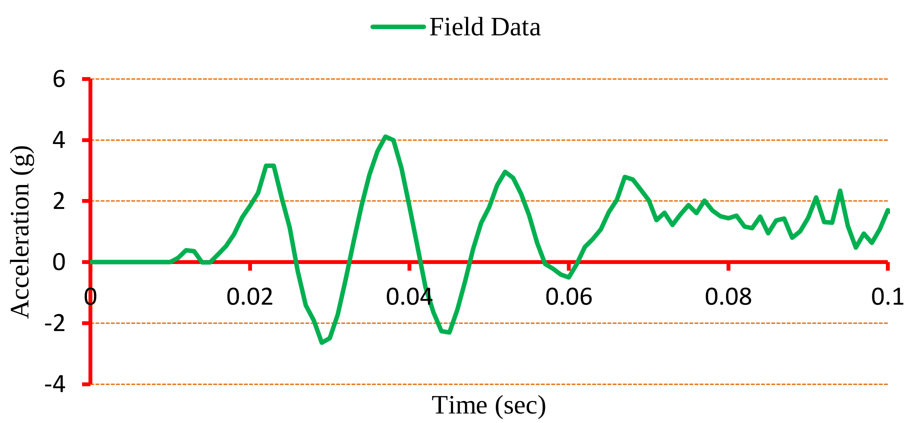

(c)

Fig. 12. Accelerations-time history chart recorded of sensor in blast experiment at (a) Foundation, (b) Floor1, and (c) Floor 2.

Figures 12a, 12b and 12c show the acceleration histories obtained from the numerical simulation with those from the structure under a 3.98 Kg equal to T.N.T charge for blast test. As displayed in According to Figure 12a, the blast wave reaches its maximum in the least amount of time. The wave is in the positive phase for 0.009 second during which it reaches the maximum acceleration of 3.48g. Then, the wave enters the negative phase, which lasts for 0.015 second during which it reaches the maximum acceleration of -3.23g.

Figures 12b and 12c show the acceleration of the floors. The acceleration in the first floor was recorded within 0.003 s since the explosion. According to Figure 12b, the maximum positive acceleration of the first floor escalated by 3.32 g within 0.013 s since the explosion. In contrast, the maximum negative acceleration intensified by 2.252 g within 0.028 s since the explosion. Then, the wave is damped over time.

Figure 12c shows the acceleration time history diagram relevant to the second floor. The maximum positive acceleration amounted to 1.4 within 0.037 s since the explosion, and the maximum negative acceleration was recorded to be -2.64 g within 0.029 s since the explosion. As shown in Figure 12c, the damage to the floor is caused by the collision of the air waves within 0.071 s since the explosion. This phenomenon is not observed in the formulation.

Now, the pressure history have to be determined to model the blast effects on the masonry structure, and then, the calculated load should be applied to the crater.

According to Eq.5, the maximum free field pressure was obtained to be 1.175 MPa, which is indeed the maximum stress on the structure. Accordingly, to determine the blast pressure history, some researchers use return analysis where different maximum stresses are applied to the blast center.

To calculate the explosion charge, it is necessary to determine P_0. However, as previously stated, no definite equation has yet been provided for the determination of P_0. Therefore, previous studies have used trial and error method which is time consuming.

To resolve this problem, FEM Updating was used in the present study. In this method, we need to define the objective function, which is defined as the difference between the recorded laboratory acceleration and the acceleration derived from numerical modeling.

The optimized parameter is considered to be the maximum free field pressure P_0. To update the model, Genetic Algorithm was utilized as an effective optimization tool. By using iterative methods in the form of the FEM updating, the physical parameters were calibrated to be able to obtain the minimum objective function value.

In the written code, the non-linear dynamic analysis program is inserted into in the Genetic algorithm as a subroutine. Then, given the upper and lower bounds specified for the optimized parameter, the numerical acceleration values are produced and compared to the field data and since the objective function is minimized, the optimized value is determined for the maximum free field pressure. To this end, the upper and lower bounds of the optimized parameter are considered to be 1 MPa and 5

MPa, respectively. After running the finite element model updating program, P_0 was determined to be 3.245 MPa. To assess the effects of the interaction between the soil and structure, the model was initially considered without soil and the structure was analyzed under the horizontal blast-induced foundation acceleration (Figure 13).

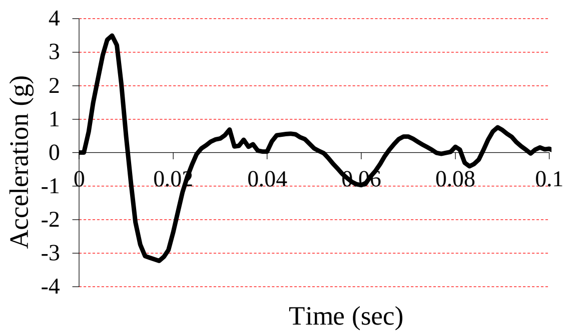

Fig. 13. Horizontal component of accelerating the foundation.

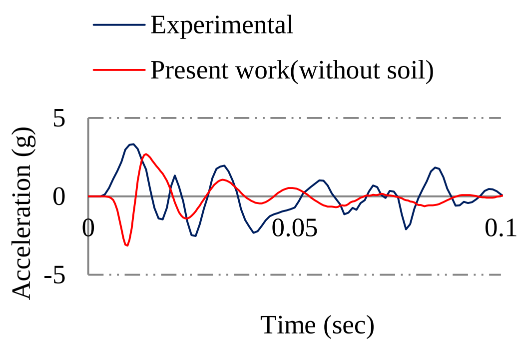

Fig.14. Horizontal component of accelerating the first floor.

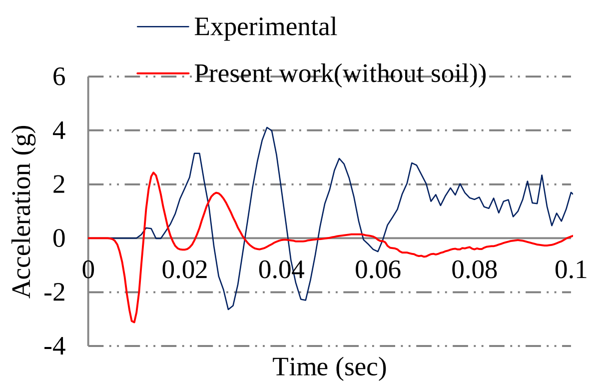

Fig. 15. Horizontal component of accelerating the second floor.

Figure. 14 represents a comparison of the first floor horizontal accelerations with and without the soil. As Figure. 15 illustrates, this difference can also be seen in the horizontal acceleration of the second floor. According to the results, the neglect of the soil- structure interaction in the numerical modeling of the buried blast leads to an error in the results.

Figures. 16, 17, and 18 show the comparisons of the acceleration histories obtained from FEM Updating results results and the field data obtained from the substructure blast.

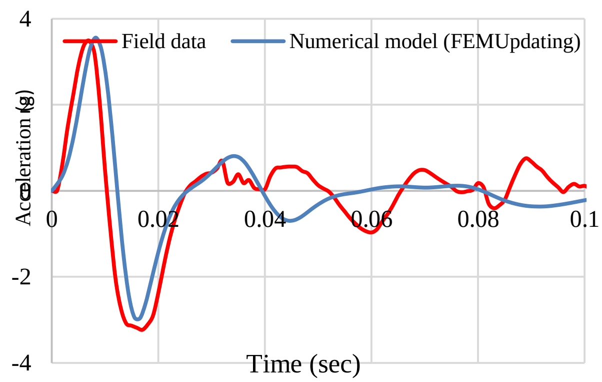

Fig. 16. The comparison between the acceleration-time history graphs received from the numerical model (FEM Updating) and the field data in the foundation.

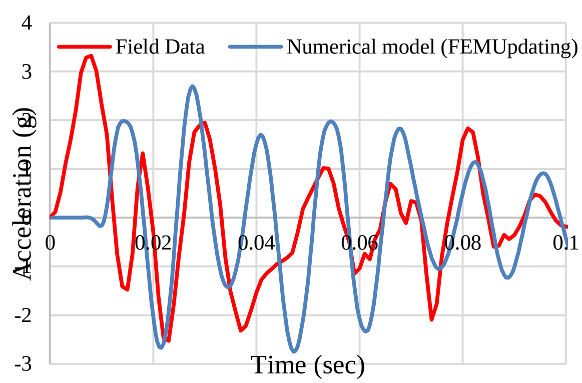

Fig. 17. The comparison between the acceleration-time history graphs received from the numerical model (FEM Updating) and the field data in the first floor.

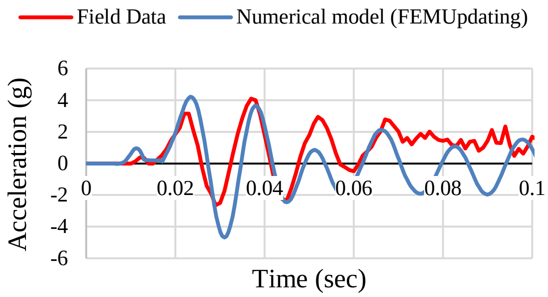

Fig. 18. The comparison between the acceleration-time history graphs received from the numerical model (FEM Updating) and the field data in the second floor.

As it is seen in Figures. 16, 17, 18, the FEM Updating results are in a good consistency with the field data.

According to the results presented in Figure. 19, the maximum pressure on the foundation is 1.21 MPa using the numerical modeling, which is in a good consistency with $P_0 = 1.17 MPa$ obtained from Eq.8.

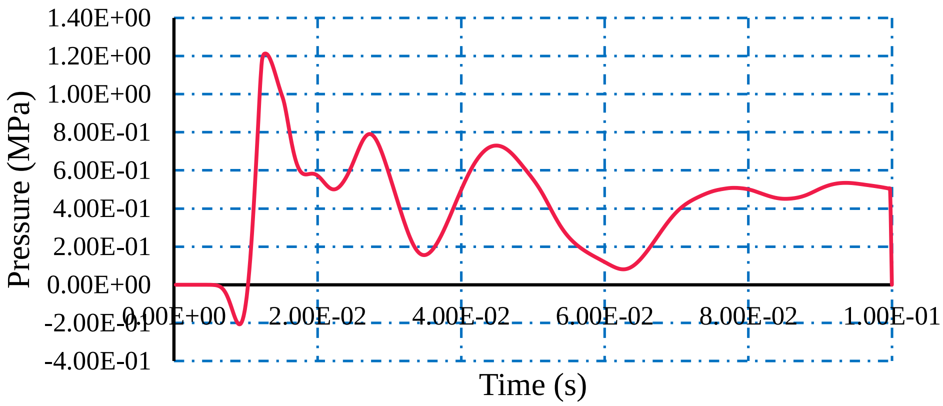

Fig. 19. Foundation pressure-time history chart obtained from numerical model.

Acknowledgment

The authors have not received any financial support from governmental and nongovernmental organizations. However, the authors are grateful to the contractor of the Jamishan Dam in Kermanshah province for sincere collaboration in performing material tests and providing a suitable site for project implementation during the Jamishan rock-fill dam construction.

6. Conclusion

Using a macro model, the present study aimed to evaluate the nonlinear dynamic response of a masonry structure via the explosion. 1.0 m × 2.2 m × 0.1 m unreinforced masonry walls were exposed to explosion loads induced by 4.5 Kg ammonium nitrate (ANFO) along with 0.428 Kg Gel-Dynamite (Emulite) (3.98 Kg equivalent T.N.T), 2 meters away from the center of the building and 1.5 meters under the ground.

The accelerations in the present research were recorded for the masonry structure. Moreover, a 3-D numerical simulation was done using the FEM code written in FORTAN to obtain acceleration distribution graphs for the masonry structure wall. The Mohr-Coulomb model with a compression-tensile cap and classic Mohr-Coulomb model were used for structure and soil modelling, respectively. An underground blast was done to produce quasi-earthquake waves.

Since the blast-induced loads are more rapid than earthquake load, the same issue leads to the local response of the structure and lower damage. Thus, the post-earthquake damage evaluation method may not be proper to assess the structures under the high frequency ground motions. Both numerical and field results can confirm the critical function of the soil-structure interaction. Reinforcement, which needs further experiments to corroborate the results, is an effective procedure to improve masonry structure responses to the blasts. Finally, the comparisons of the FEM Updating results and field data highlight the method's potential for the blast numerical modeling.

The results of the present study showed that the FEM updating can be used for explosion modeling instead of time-consuming recursive analysis to calculate the maximum free-field pressure.

REFERENCES

[1] Sielicki, P.W., "Masonry failure under unusual impulse loading." 2013: Wydawnictwo Politechniki PoznaĹ„skiej.

[2] Wu, C., H. Hao, and Y. Lu, "Dynamic response and damage analysis of masonry structures and masonry infilled RC frames to blast ground motion." Engineering Structures, 2005. 27(3): p. 323-333.

[3] Chen, L., et al., "Responses of masonry infill walls retrofitted with CFRP, steel wire mesh and laminated bars to blast loadings." Advances in Structural Engineering, 2014. 17(6): p. 817-836.

[4] Chen, L., et al. "Calibration and discussion of parameters of Mat_72Rel3 constitutive model on clay brick and mortar materials." in Proceedings of 15th International Symposium on the Interaction of the Effects of Munitions with Structures. 2013.

[5] Gebbeken, N., T. Linse, and T. Araújo, "Masonry under dynamic actions—experimental investigations, material modeling and numerical simulations." Advances in Protective Structures Research, 2012. 1: p. 131.

[6] Meyer, M.C.S., "Development of brick and mortar material parameters for numerical simulations, in Dynamic Behavior of Materials." Volume 1. 2011, Springer. p. 351-359.

[7] Wei, X. and M.G. Stewart, "Model validation and parametric study on the blast response of unreinforced brick masonry walls." International journal of impact engineering, 2010. 37(11): p. 1150-1159.

[8] Ma, G., H. Hao, and Y. Lu, "Homogenization of masonry using numerical simulations." Journal of engineering mechanics, 2001. 127(5): p. 421-431.

[9] Milani, G., P.B. Lourenço, and A. Tralli, "Homogenized rigid-plastic model for masonry walls subjected to impact." International Journal of Solids and Structures, 2009. 46(22): p. 4133-4149.

[10] Wei, X. and H. Hao, "Numerical derivation of homogenized dynamic masonry material properties with strain rate effects." International Journal of Impact Engineering, 2009. 36(3): p. 522-536.

[11] Wu, C. and H. Hao, "Derivation of 3D masonry properties using numerical homogenization technique." International Journal for numerical methods in engineering, 2006. 66(11): p. 1717-1737.

[12] Keys, R. and S.K. Clubley, "Modelling debris distribution of masonry panels subject to blast loads using experimental & applied element methods." 2013.

[13] Riedel, W., et al., "Modeling and validation of a wall-window retrofit system under blast loading." Engineering Structures, 2012. 37: p. 235-245.

[14] Akhaveissy, A., et al., "Implementation and comparison of a generalized plasticity and disturbed state concept for the load-deformation behavior of foundations."

Scientia Iranica, Transaction A: Civil Engineering, 2009. 16(3): p. 189-198.

[15] Akhaveissy, A., “Evaluation of Tunnel-Structure Interaction due to Strong ground movement.” 2007, Ph. D. Thesis, Civil Engineering Department, Tarbiat Modares University, Tehran, Iran.

[16] Akhaveissy, A., “Analysis of tunnel and super structures for excavation.” Scientia Iranica, 2011. 18(1): p. 1-8.

[17] Tu, Z. and Y. Lu, “FE model updating using artificial boundary conditions with genetic algorithms.” Computers & Structures, 2008. 86(7-8): p. 714-727.

[18] Wang, Z.-C., Y. Xin, and W.-X. Ren, “Nonlinear structural model updating based on instantaneous frequencies and amplitudes of the decomposed dynamic responses.” Engineering Structures, 2015. 100: p. 189-200.

[19] Xu, Y., et al., “Probability-based damage detection using model updating with efficient uncertainty propagation.” Mechanical Systems and Signal Processing, 2015. 60: p. 958-970.

[20] Bakir, P.G., E. Reynders, and G. De Roeck, “Sensitivity-based finite element model updating using constrained optimization with a trust region algorithm.” Journal of Sound and Vibration, 2007. 305(1-2): p. 211-225.

[21] Bartoli, G., et al., “Bayesian model updating of historic masonry towers through dynamic experimental data.” Procedia engineering, 2017. 199: p. 1258-1263.

[22] Schlune, H., M. Plos, and K. Gylltoft, “Improved bridge evaluation through finite element model updating using static and dynamic measurements.” Engineering structures, 2009. 31(7): p. 1477-1485.

[23] Minshui, H. and Z. “Hongping, Finite element model updating of bridge structures based on sensitivity analysis and optimization algorithm.” Wuhan University Journal of Natural Sciences, 2008. 13(1): p. 87-92.

[24] Cooper, P.W., “Explosives engineering.” 1996: Vch Pub.

[25] Standard, A., “Standard test method for consolidated undrained triaxial compression test for cohesive soils.” ASTM International 2002, ASTM D4767, 2002. 2.

[26] Jayasinghe, L.B., et al., “Blast response and failure analysis of pile foundations subjected to surface explosion.” Engineering Failure Analysis, 2014. 39: p. 41-54.

[27] Saleh, M. and L. Edwards, “Evaluation of soil and fluid structure interaction in blast modelling of the flying plate test.” Computers & Structures, 2015. 151: p. 96-114.

[28] Fox, D., et al., “The response of small scale rigid targets to shallow buried explosive detonations.” International Journal of Impact Engineering, 2011. 38(11): p. 882-891.

[29] Neuberger, A., S. Peles, and D. Rittel, “Scaling the response of circular plates subjected to large and close-range spherical explosions.” Part II: buried charges. International Journal of Impact Engineering, 2007. 34(5): p. 874-882.

[30] Tian, L. and Z.-X. Li, “Dynamic response analysis of a building structure subjected to ground shock from a tunnel explosion.” International Journal of Impact Engineering, 2008. 35(10): p. 1164-1178.

[31] Akhaveissy, A. and G. Milani, “Pushover analysis of large scale unreinforced masonry structures by means of a fully 2D non-linear model.” Construction and Building Materials, 2013. 41: p. 276-295.

[32] Hyde, D., “User’s guide for microcomputer program CONWEP, application of TM5-855-1, fundamentals of protective design for conventional weapons.” Instructional Rep. No. SL-88, 1992. 1.